

UBVI CCD photometry and star counts in nine inner disk Galactic star clusters^{*}

Giovanni Carraro^{1†‡} and Anton F. Seleznev^{2§}

¹European Southern Observatory, Alonso de Cordova 3107, Casilla 19001, Santiago 19, Chile

²Astronomical Observatory, Ural State University, Lenin Avenue. 51, Ekaterinburg 620083, Russia

Accepted 2011..... Received 2011...; in original form 2011...

ABSTRACT

We present and discuss new CCD-based photometric material in the UBVI pass-bands for nine Galactic star clusters located inside the solar ring, for which no CCD data are currently available. They are: IC 2714, NGC 4052, ESO131SC09, NGC 5284, NGC 5316, NGC 5715, VdB-Hagen 164, NGC 6268, and Czernik 38. The main aim of this study is to establish their nature of real clusters or random field star enhancements and, when real, estimate their fundamental parameters. To this aim, we first perform star counts by combining our optical photometry with 2MASS, and derive cluster sizes and radial density profiles. The fundamental parameters - age, reddening and distance- are then inferred from the analysis of the star distribution in color-color and color-magnitude diagrams of only the spatially selected likely members. Our analysis shows that ESO131SC09, NGC 5284, and VdB-Hagen 164 are most probably not clusters, but random enhancements of a few bright stars along the line of sight, with properties much similar to so-called open cluster remnants. The remaining clusters are physical groups, and are all younger than about 1 Gyr. We use the newly derived set of parameters, in particular distance and reddening, to investigate their position in the Galaxy in the context of the spiral structure of the Milky Way. We find that the youngest clusters (IC 2714, NGC 5316, and NGC 6268) are located close to or inside the Carina-Sagittarius arm, and are therefore *bona fide* spiral structure tracers. On the other hand, the oldest (Czernik 38, NGC 4052, and NGC 5715) are floating in the inter-arm space between the Carina-Sagittarius and the more distant Scutum-Crux arm. Interestingly enough, the oldest clusters of this sample - Czernik 38 and NGC 5715- are among the few known open clusters to be older or as old as the Hyades in the inner Galactic disk, where star clusters are not expected to survive for a long time, because of the strong tidal field and the higher probability of close encounters.

Key words: open clusters and associations: general - open clusters and associations: individual: photometry Galaxy: disc Galaxy: spiral structure

1 INTRODUCTION

In the Milky Way, stellar clusters form in dense regions located inside spiral arms. When clusters survive, they remain connected with the parent arm for about 100 Myr (Dobbs & Pringle 2010). Afterwards they decouple from it and are no longer useful as spiral structure tracers. Young star clusters have been used for half a century to probe the spiral structure of the Milky Way (MW). Historically, the first arms to be detected using young open clusters, were the Perseus arm in the second galactic quadrant, the Carina-Sagittarius in the fourth quadrant, and the Orion spur in which the

Sun is embedded (Trumpler 1930). Nowadays, the picture we have of the MW spiral structure contains many more details (Russeil 2003, Efremov 2011, Lepine et al. 2011), although a lively discussion is still ongoing as to how many major arms are present and if they are long-lived or transient (Grosbol et al. 2011).

In the last decade, young star clusters played a major role in improving our knowledge of the MW spiral structure, especially in the third Galactic quadrant. Moitinho et al. (2005), Vazquez et al. (2008) and Carraro et al. (2010) identified for the first time in optical observations the outer Norma-Cygnus arm, and clarified the shape and interaction of the Orion and Perseus arms. These studies made clear that young star clusters are powerful spiral tracers when it is possible to determine their distance and age with high confidence. In particular, the authors stress how crucial deep *U*-band photometry is to pin down cluster reddening and hence obtain their distance.

^{*} Based on observations collected at the Cerro Tololo Inter-American Observatory and Las Campanas Observatory, Chile.

[†] On leave from Dipartimento di Astronomia, Università di Padova, Italy

[‡] E-mail: gcarraro@eso.org (GC); anton.seleznev@usu.ru (AFS)

[§] ESO Visiting Scientist

We also present and discuss *UBVI* photometry of nine star clusters all located in the fourth Galactic quadrant except for one - Czernik 38-, which is located in the first quadrant (see Table 1). Most of them are nothing more than simple star cluster candidates, according to most public catalogs, and do not have any published data. However, we expect that they are mostly young clusters based both on inspection of DSS maps and on the widely spread idea that clusters cannot survive for a long time in the inner Galactic disk.

Apart from the obvious goal to establish their nature and derive their fundamental parameters, we aim to use them - when they are sufficiently young- as spiral arm tracers in the longitude range $290^\circ \leq l \leq 360^\circ$. In this MW sector, inside the solar ring, we expect the lines of sight of the clusters to first encounter the Carina-Sagittarius arm, and hopefully, also the Scutum-Crux arm, which is much closer to the Galactic Center, as well as the Perseus arm, which is much further away (Vázquez et al. 2005; Carraro & Costa 2009; Baume et al. 2009).

The technique we used is based on the analysis of the color-color and color-magnitude diagrams of groups of stars properly selected after having performed star counts and defined clusters' reality and size (see Seleznev et al. 2010 for details).

As a consequence, the paper is organized as follows:

In Sect. 2 we present information culled from literature on the objects under investigation, which demonstrate they have been almost completely overlooked in the past. Sect. 3 presents the observations and basic data reduction, together with photometric calibration, completeness analysis and cross-correlation with 2MASS. The comparison with previous photometry - when available- are discussed in Sections 4. Section 5 is devoted to star counts and the derivation of clusters' size. We then estimate the method to infer clusters' fundamental parameters in Sect. 6. Sect. 7, finally, discusses the outcome of this analysis. The conclusions of this investigation, together with suggestions/recommendations for further studies, are provided in Sect. 8.

2 PREVIOUS INVESTIGATIONS

Most clusters in the sample we investigated for this paper have not been studied so far, and only for one -Czernik 38- some preliminary CCD data have been provided.

We present here a compilation of any previous study we could find in the literature to date, on a cluster-by-cluster basis.

IC 2714

This is the star cluster of the whole sample which received more attention in the past. We selected this cluster also as a control object for our photometry, which we are going to compare in Sect. 4.

UBV photo-electric photometry of about 200 stars have been presented by Claria et al. (1994), together with spectroscopy of 14 probable giant star members of the cluster. These authors derived an age of 300 million years and place the cluster at a distance of 1300 pc, in agreement with previous findings by Becker (1960). They found that the cluster suffers from variable extinction, and obtain $E(B-V)=0.36$ from the turnoff, and 0.37 from giant stars. As for the metallicity, they found a large range of value, from +0.05 using DDO to -0.18 using Washington photometric system. A revision of the DDO calibration led Twarog et al (1997) to

provide $[Fe/H]$ ranging from -0.01 to 0.02, and $E(B-V)=0.35$. More recently, spectroscopic analysis by Santos et al. (2009) confirmed the range of metallicity found by Twarog et al. (1997), ruling out the results of the Washington photometry. Finally, Smiljanic et al (2009) derived $[Fe/H]=0.12$ from one giant, and reddening $E(B-V)=0.33$. By adopting Shaller et al (1992) isochrones, they fit Claria et al (1994) photometry, getting an apparent distance modulus $(m-M)=11.5$, and an age of 400 million years.

NGC 4052

van den Berg & Hagen (1975) describe NGC 4052 as a medium richness, real cluster, mostly composed of blue stars, and possibly embedded in some nebosity. The shallow study of Kharchenko et al. (2005) provides preliminary estimates of the cluster parameters based on photometry and astrometry of less than 20 stars brighter than $V \sim 12$. They locate this 250 million years old cluster at 1200 pc from the Sun. No CCD studies of NGC 4052 have been conducted so far.

ESO-131SC09

No information is available for this cluster apart from its size, which is around 5 arcmin according to Dias et al. (2002).

NGC 5284

No information is available for this cluster beyond the mere classification.

NGC 5316

The only available study for this cluster is the photo-electric investigation by Ramin (1966) down to $V \sim 16$, which places the cluster at an heliocentric distance of 1200 pc. The age of 150 million is derived by Kharchenko et al. (2005) from a subsample of stars brighter than $V \sim 12$. Its young age is also recognized by the visual inspection of van den Berg & Hagen (1975).

NGC 5715

van den Berg & Hagen (1975) describe NGC 5715 as a medium richness, real cluster, mostly composed of blue stars. No optical study is available for NGC 5715, whose properties have been however investigated using 2MASS by Bonatto & Bica (2007). They report an age of 800 million years and a distance of 1.5 kpc from the Sun.

Vdb-Hagen 164

van den Berg & Hagen (1975) describe this cluster as a very poor ensemble of blue stars. No data is available for it to date.

NGC 6268

Seggewiss (1968) provided some photographic photometry of NGC 6268 down to $V \sim 14$, and its analysis led to an helio-centric distance of 1200 pc. Later, van den Berg & Hagen (1975) described it as a very poor ensemble of blue stars. The shallower study by Kharchenko et al. (2005) found a somewhat smaller distance of 1000 pc, and suggests an age around 15 million years, lending support to van den Berg & Hagen's (1975) visual impressions.

Czernik 38

Discovered by Czernik (1966), this cluster is described as a relatively rich cluster with a diameter of 14 arcmin. Schmidt camera CCD photometry has been recently obtained by Maciejewski (2008). This author suggests that the cluster is at least 1 Gyr old,

Table 1. Basic parameters of the clusters under investigation. Coordinates are for J2000.0. In the last two columns we report the extinction at infinity and the Observatory where data were taken.

Number	Name	<i>RA</i>	<i>DEC</i>	<i>l</i>	<i>b</i>	E(B-V)	Observatory
		<i>hh : mm : ss</i>	<i>° : ' : ''</i>	[deg]	[deg]	mag	
1	IC 2714	11:17:27.0	-62:44:00.0	292.40	-1.799	2.77	LCO
2	NGC 4052	12:01:12.0	-63:13:12.0	297.30	-0.900	4.15	LCO
3	ESO131SC09	12:29:37.4	-57:52:31.0	300.02	4.873	0.87	CTIO
4	NGC 5284	13:46:29.9	-59:08:39.0	309.95	2.975	1.25	CTIO
5	NGC 5316	13:53:57.0	-61:52:06.0	310.23	0.115	12.02	LCO
6	NGC 5715	14:43:29.0	-57:34:36.0	317.53	2.085	1.78	LCO
7	VdB-Hagen 164	14:48:13.7	-66:20:12.0	314.28	-6.070	0.32	CTIO
8	NGC 6268	17:02:00.8	-39:44:18.0	346.10	1.216	5.81	CTIO
9	Czernik 38	18:49:42.0	+05:52:00.0	37.13	2.630	2.08	CTIO

and places it at an helio-centric distance of 1200 pc.

3 OBSERVATIONS

In this section we describe in details how we conducted observations and reduced the collected data. Five of the program clusters (ESO131SC09, NGC 5284, VdB-Hagen 164, NGC 6268, and Czernik 38) were surveyed at CTIO (Cerro Tololo Inter-American Observatory¹), while the remaining four (IC 2714, NGC 4052, NGC 5316 and NGC 5715) were imaged at LCO (Las Campanas Observatory²). Their Equatorial and Galactic coordinates for the 2000.0 equinox are reported in Table 1, together with an estimate of the reddening from FIRB (Schlegel et al. 1998). The last column indicates where each cluster was observed. Fig 1, finally, shows DSS images of the nine fields where the clusters are located.

Because of the differences in both telescopes and detectors, we will describe separately the observations and data reduction of the two clusters' groups.

3.1 CTIO Observations

These regions were observed with the Y4KCam camera attached to the Cerro Tololo Inter-American Observatory (CTIO) 1-m telescope, operated by the SMARTS consortium.³ This camera is equipped with an STA 4064×4064 CCD⁴ with 15-μm pixels, yielding a scale of 0.289''/pixel and a field-of-view (FOV) of 20' × 20' at the Cassegrain focus of the CTIO 1-m telescope. The CCD was operated without binning, at a nominal gain of 1.44 e⁻/ADU, implying a readout noise of 7 e⁻ per quadrant (this detector is read by means of four different amplifiers).

In Table 2 we present the log of our *UBVI* observations. All observations were carried out in photometric, good-seeing (always less than 1.2 arcsec), conditions. Our *UBVI* instrumental photometric system was defined by the use of a standard broad-band Kitt

Peak *UBVI*_{ke} set of filters.⁵ To determine the transformation from our instrumental system to the standard Johnson-Kron-Cousins system, and to correct for extinction, we observed stars in Landolt's areas PG 1047, PG 1323, G 26 and MarkA (Landolt 1992) multiple times and with different air-masses ranging from ~ 1.03 to ~ 2.0 , and covering quite a large color range $-0.3 \leq (B - V) \leq 2.0$ mag.

3.2 LCO Observations

Four clusters were observed at LCO (see Table 1) on the nights of May 8 to 10, 2010, as illustrated in Table 3. The clusters were observed using the SITE#3 CCD detector onboard the Swope 1.0m telescope. With a pixel scale of 0.435 arcsec/pixel, this CCD allows to cover 14.8×22.8 arcmin on sky. To determine the transformation from our instrumental system to the standard Johnson-Kron-Cousins system, and to correct for extinction, we observed stars in Landolt's areas PG 1047, PG 1323, PG 1633, PG 1657, and MarkA (Landolt 1992) multiple times and with different air-masses ranging from ~ 1.05 to ~ 1.9 , and covering quite a large color range $-0.4 \leq (B - V) \leq 2.1$ mag (see Table 3). We secured night-dependent calibrations.

3.3 Photometric reductions

Basic calibration of the CCD frames was done using IRAF⁶ package CCDRED. For this purpose, zero exposure frames and twilight sky flats were taken every night. Photometry was then performed using the IRAF DAOPHOT/ALLSTAR and PHOTCAL packages. Instrumental magnitudes were extracted following the point-spread function (PSF) method (Stetson 1987). A quadratic, spatially variable, master PSF (PENNY function) was adopted, because of the large field of view of the two detectors. Aperture corrections were then determined making aperture photometry of a suitable number (typically 10 to 20) of bright, isolated, stars in the field. These corrections were found to vary from 0.160 to 0.290 mag, depending on the filter. The PSF photometry was finally aperture corrected, filter by filter.

¹ <http://www.ctio.noao.edu>

² <http://www.lco.cl>

³ <http://http://www.astro.yale.edu/smarts>

⁴ <http://www.astronomy.ohio-state.edu/Y4KCam/detector.html>

⁵ <http://www.astronomy.ohio-state.edu/Y4KCam/filters.html>

⁶ IRAF is distributed by the National Optical Astronomy Observatory, which is operated by the Association of Universities for Research in Astronomy, Inc., under cooperative agreement with the National Science Foundation.

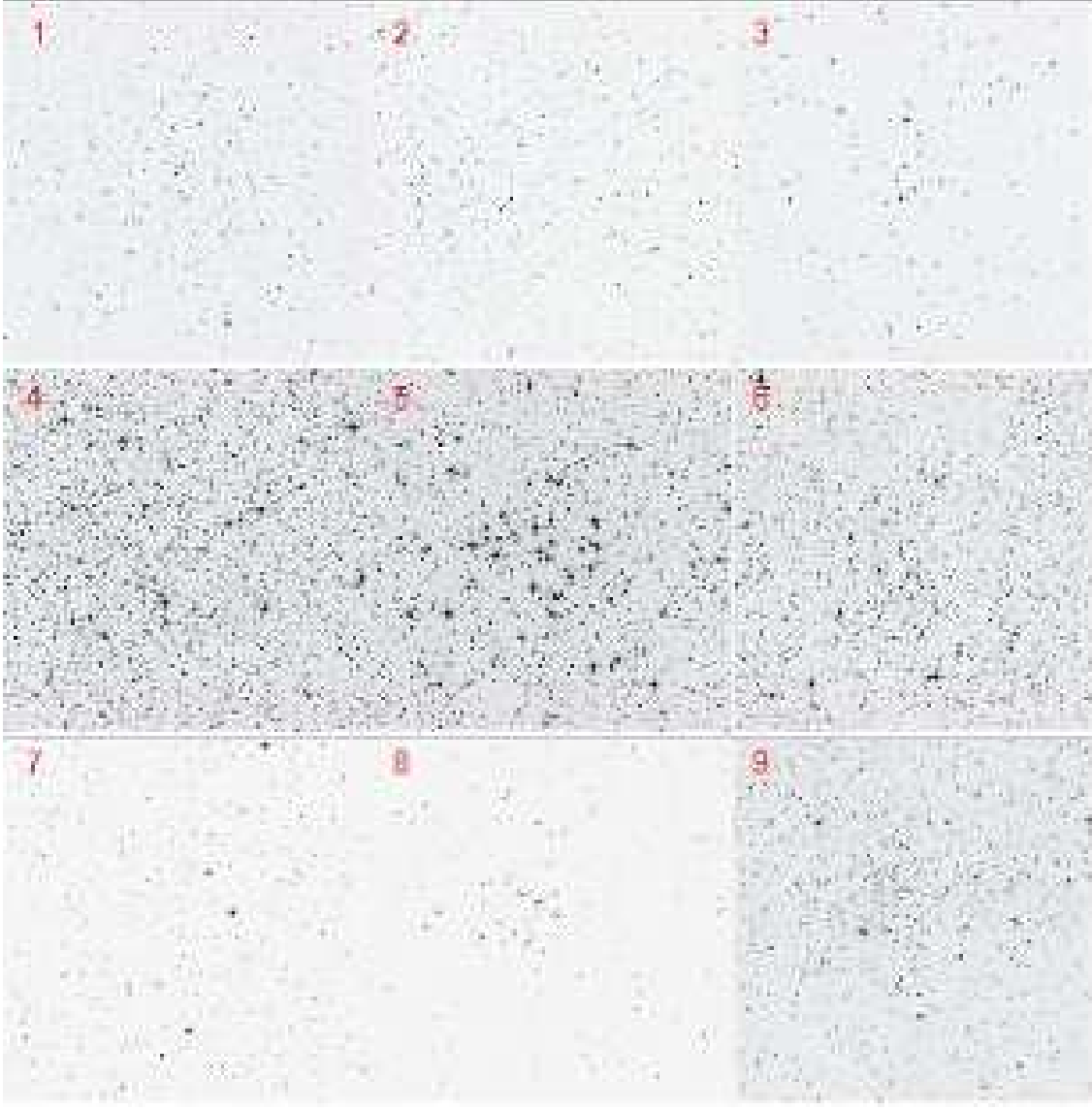


Figure 1. DSS images centered on the 9 program clusters. North is up, East to the left, and the field of view is 20 arcmin on a side. Images follow the numbering in Table 1 from top left to bottom right.

3.4 Photometric calibration

After removing problematic stars, and stars having only a few observations in Landolt's (1992) catalog, our photometric solution for the CTIO run was extracted from a grand total of 92 measurements per filter, and turned out to be:

$$\begin{aligned}
 U &= u + (3.110 \pm 0.010) + (0.45 \pm 0.01) \times X - (0.010 \pm 0.006) \times (U - B) \\
 B &= b + (2.143 \pm 0.012) + (0.27 \pm 0.01) \times X - (0.118 \pm 0.007) \times (B - V) \\
 V &= v + (1.740 \pm 0.007) + (0.15 \pm 0.01) \times X + (0.038 \pm 0.007) \times (B - V) \\
 I &= i + (2.711 \pm 0.011) + (0.08 \pm 0.01) \times X + (0.041 \pm 0.008) \times (V - I)
 \end{aligned}$$

The final *r.m.s* of the fitting was 0.030, 0.015, 0.010, and 0.010 in

U , B , V and I , respectively.

As for LCO observations, we provided individual night-based photometric solutions. However, since the three solutions were identical, we merged and averaged them together in a single photometric solution. This implies a grand total of 103 measures per filter, and the solutions read:

$$\begin{aligned}
 U &= u + (4.902 \pm 0.010) + (0.41 \pm 0.01) \times X + (0.129 \pm 0.020) \times (U - B) \\
 B &= b + (3.186 \pm 0.012) + (0.31 \pm 0.01) \times X + (0.057 \pm 0.008) \times (B - V) \\
 V &= v + (3.115 \pm 0.007) + (0.17 \pm 0.01) \times X - (0.057 \pm 0.011) \times (B - V) \\
 I &= i + (3.426 \pm 0.011) + (0.07 \pm 0.01) \times X + (0.091 \pm 0.012) \times (V - I)
 \end{aligned}$$

The final *r.m.s* of the fitting in this case was 0.040, 0.025,

Table 2. *UBVI* photometric observations of star clusters and standard star fields for the CTIO run.

Target	Date	Filter	Exposure (sec)	airmass
PG 1047	2006 May 21	<i>U</i>	90,180	1.15–1.25
		<i>B</i>	2x80	1.15–1.21
		<i>V</i>	2x50	1.14–1.16
		<i>I</i>	2x50	1.15–1.15
ESO131SC09	2006 May 21	<i>U</i>	30, 200, 1500	1.13–1.13
		<i>B</i>	30, 100, 1200	1.14–1.16
		<i>V</i>	30, 100, 900	1.14–1.15
		<i>I</i>	30, 100, 700	1.13–1.14
NGC 5284	2006 May 21	<i>U</i>	30, 200, 1500	1.15–1.15
		<i>B</i>	30, 100, 1200	1.16–1.15
		<i>V</i>	30, 100, 900	1.15–1.15
		<i>I</i>	30, 100, 700	1.15–1.15
PG 1323	2006 May 21	<i>U</i>	2x150	1.15–1.14
		<i>B</i>	80	1.13–1.14
		<i>V</i>	50	1.15–1.15
		<i>I</i>	50	1.14–1.14
VdB-Hagen154	2006 May 21	<i>U</i>	30, 200, 1500	1.25–1.25
		<i>B</i>	30, 100, 1200	1.26–1.25
		<i>V</i>	30, 100, 900	1.25–1.25
		<i>I</i>	30, 100, 700	1.25–1.25
NGC 6268	2006 May 21	<i>U</i>	30, 200, 1500	1.15–1.15
		<i>B</i>	30, 100, 1200	1.16–1.15
		<i>V</i>	30, 100, 900	1.15–1.15
		<i>I</i>	30, 100, 700	1.15–1.15
MarkA	2006 May 21	<i>U</i>	100, 150, 180	1.05–1.94
		<i>B</i>	3x80	1.03–1.84
		<i>V</i>	3x50	1.05–1.85
		<i>I</i>	3x50	1.04–1.99
Czernik 38	2006 May 21	<i>B</i>	30, 100, 1200	1.46–1.45
		<i>V</i>	10, 30, 100, 900	1.45–1.45
		<i>I</i>	30, 100, 700	1.45–1.45
G 26	2006 May 21	<i>U</i>	100, 150	1.35–1.74
		<i>B</i>	2x80	1.33–1.77
		<i>V</i>	2x50	1.35–1.75
		<i>I</i>	2x50	1.34–1.79

0.015, and 0.015 in *U*, *B*, *V* and *I*, respectively.

Global photometric errors were estimated using the scheme developed by Patat & Carraro (2001, Appendix A1), which takes into account the errors resulting from the PSF fitting procedure (i.e., from ALLSTAR/ALLFRAME), and the calibration errors (corresponding to the zero point, colour terms, and extinction errors). In Fig. 2 we present our global photometric errors in *V*, $(B - V)$, $(U - B)$, and $(V - I)$ plotted as a function of *V* magnitude. Quick inspection shows that stars brighter than $V \approx 20$ mag have errors lower than ~ 0.05 mag in magnitude and lower than ~ 0.10 mag in $(B - V)$ and $(V - I)$. Higher errors are seen in $(U - B)$.

Our CTIO final optical photometric catalogs consist of 4432, 8485, 12464, 1163, and 3892 entries having *UBVI* measurements down to $V \sim 22$ mag for ESO131SC09, NGC 5284, VdB-Hagen 164, NGC 6268, and Czernik 38, respectively. As for LCO, the catalogs for IC 2714, NGC 4052, NGC 5316 and NGC 5715 report 2756, 6650, 2524, and 4105 *UBVI* entries. These catalogs will be made

Table 3. *UBVI* photometric observations of star clusters and standard star fields for the LCO run

Target	Date	Filter	Exposure (sec)	airmass
IC 2714	2010 May 08	<i>U</i>	10, 300, 1500	1.28–1.35
		<i>B</i>	10, 200, 1200	1.25–1.26
		<i>V</i>	3, 30, 900	1.23–1.23
		<i>I</i>	3, 10, 900	1.21–1.23
MarkA	2010 May 08	<i>U</i>	2x240	1.07–1.38
		<i>B</i>	2x180	1.07–1.41
		<i>V</i>	2x60	1.07–1.43
		<i>I</i>	40,50	1.07–1.43
PG 1047	2010 May 08	<i>U</i>	20,180	1.14–1.91
		<i>B</i>	15,180	1.14–1.88
		<i>V</i>	2x10,20,30	1.15–1.83
		<i>I</i>	10,30	1.15–1.86
PG 1323	2010 May 08	<i>U</i>	180	1.11–1.11
		<i>B</i>	120	1.12–1.12
		<i>V</i>	30	1.15–1.15
		<i>I</i>	30	1.14–1.14
NGC 4052	2010 May 09	<i>U</i>	10, 300, 1500	1.28–1.35
		<i>B</i>	10, 200, 1200	1.21–1.22
		<i>V</i>	3, 30, 900	1.23–1.24
		<i>I</i>	3, 10, 900	1.22–1.22
NGC 5316	2010 May 09	<i>U</i>	10, 300, 1500	1.17–1.20
		<i>B</i>	10, 200, 1200	1.22–1.22
		<i>V</i>	3, 30, 900	1.23–1.24
		<i>I</i>	3, 10, 900	1.19–1.19
MarkA	2010 May 09	<i>U</i>	240	1.30–1.30
		<i>B</i>	180	1.33–1.33
		<i>V</i>	60	1.28–1.28
		<i>I</i>	60	1.26–1.26
PG 1633	2010 May 09	<i>U</i>	90,120	1.29–1.72
		<i>B</i>	60,90	1.29–1.74
		<i>V</i>	30,40,90	1.29–1.76
		<i>I</i>	30,40	1.29–1.78
PG 1323	2010 May 09	<i>U</i>	3x25, 60	1.07–1.88
		<i>B</i>	2x20, 26, 60	1.07–1.71
		<i>V</i>	10, 3x15, 2x30	1.07–1.79
		<i>I</i>	3x15, 30	1.07–1.74
NGC 5715	2010 May 10	<i>U</i>	10, 300, 1500	1.19–1.19
		<i>B</i>	10, 200, 1200	1.25–1.26
		<i>V</i>	3, 30, 900	1.19–1.20
		<i>I</i>	3, 10, 900	1.21–1.22
PG 1323	2010 May 10	<i>U</i>	2x25	1.07–1.22
		<i>B</i>	2x20	1.07–1.22
		<i>V</i>	2x10	1.07–1.20
		<i>I</i>	2x10	1.07–1.20
PG 1657	2010 May 10	<i>U</i>	2x180	1.29–1.49
		<i>B</i>	2x120	1.29–1.52
		<i>V</i>	2x60	1.30–1.54
		<i>I</i>	2x60	1.30–1.56

available at the WEBDA⁷ data-base maintained by E. Paunzen at Vienna University, Austria.

3.5 Completeness and astrometry

Completeness corrections were determined by running artificial star experiments on the data. Basically, we created several artificial images by adding artificial stars to the original frames. These stars

⁷ <http://www.univie.ac.at/webda/navigation.html>

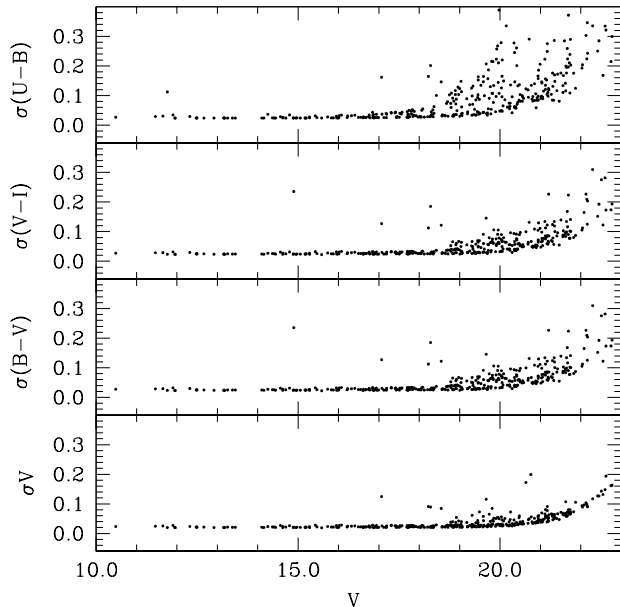


Figure 2. Photometric errors in V , $(B - V)$, $(V - I)$, and $(U - B)$, as a function of the V magnitude.

were added at random positions, and had the same colour and luminosity distribution of the true sample. To avoid generating overcrowding, in each experiment we added up to 25% of the original number of stars. Depending on the frame, between 1000 and 5000 stars were added. In this way we have estimated that the completeness level of our photometry is better than 90% down to $V = 19.5$.

Each optical catalog was then cross-correlated with 2MASS, which resulted in a final catalog including $UBVI$ and JHK_s magnitudes. As a by-product, pixel (i.e., detector) coordinates were converted to RA and DEC for J2000.0 equinox, thus providing 2MASS-based astrometry, useful for *e.g.* spectroscopic follow-up.

4 COMPARISON WITH PREVIOUS PHOTOMETRY

The only cluster in our sample having previous CCD photometry is Czernik 38, for which BV photometry was provided by Maciejewski (2008). We can only compare BV, since Maciejewski did not observe in I. We found 425 stars in common, and the results are shown in Fig 3, in the sense of our photometry minus Maciejewski. We found that the two studies are very different both in V and in B mag. The mean differences are reported in the top left corners of the various panels in Fig. 3. The reasons for such important zero point differences can be various. We remind the reader that Maciejewski observed in very poor seeing conditions (~ 4 arcsec) and with a Schmidt camera having a scale as large as 1.08 arcsec/pixel. Besides, the color range of the standard stars is limited between 0.3 and 1.3 in B-V, while all Main Sequence stars in Czernik 38 have redder colors. This implied he had to extrapolate colors when calibrating. Besides, with such a poor detector scale, the seeing conditions and moderated crowding of the field (see Fig. 1) easily produce blends, and stars tend, on the average, to be brighter. This is exactly what the positive residuals

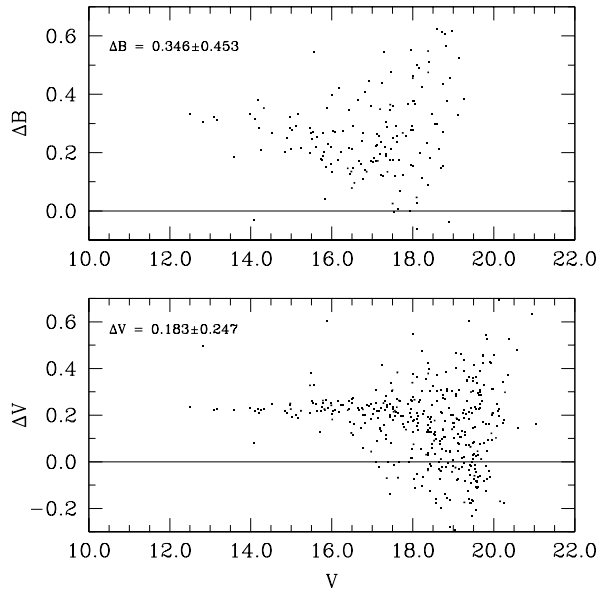


Figure 3. Comparison of our photometry for Czernik 38 with Maciejewski (2008) for V and B . The comparison is in the sense of our photometry versus theirs.

in Fig. 3 indicate. For all these reasons we believe our photometry is more solid and precise (note the scatter in the residual in Fig 3 for V larger than ~ 17.0 mag).

To further check the quality of our data, we compared our UBV photometry for IC 2714 with the higher quality photoelectric study by Clariá et al. (1994). This is shown in Fig. 4. The comparison is done for 90 common stars and it is in the sense of our photometry minus Clariá et al. (1994). The results are quite good for V and $B-V$, as indicated in Fig. 4, down to $V \sim 14.0$. However, we found some discrepancy for $U-B$, in the form of a un-accounted color term.

5 STAR COUNTS, CLUSTERS' REALITY AND SIZE.

In this section we make use of our photometric data-set, and of infra-red photometry from the 2MASS data-base, to perform star counts in the area of the program clusters, assess their reality, and derive estimates of their radii.

5.1 Surface Density Maps and Cluster Center Coordinates

Surface Density Maps (SDM) were constructed for all fields under investigation to determine the cluster's reality and size. Examples of the application of this technique can be found in Prisinzano et al. (2001), Pancino et al.(2003), and Seleznev et al (2010), which the reader is referred to for any additional details.

Briefly, SDM were constructed using the kernel estimation method (see *e.g.* Silverman 1986), with a kernel half-width of 400 pixel s(corresponding to $2.90'$ for LCO clusters and $1.93'$ for CTIO clusters). Moreover, a grid of 20-pixel cells for LCO clusters, and of 50-pixel cells for CTIO clusters, were adopted. The large kernel half-width (HW) was chosen in order to both decrease the effect

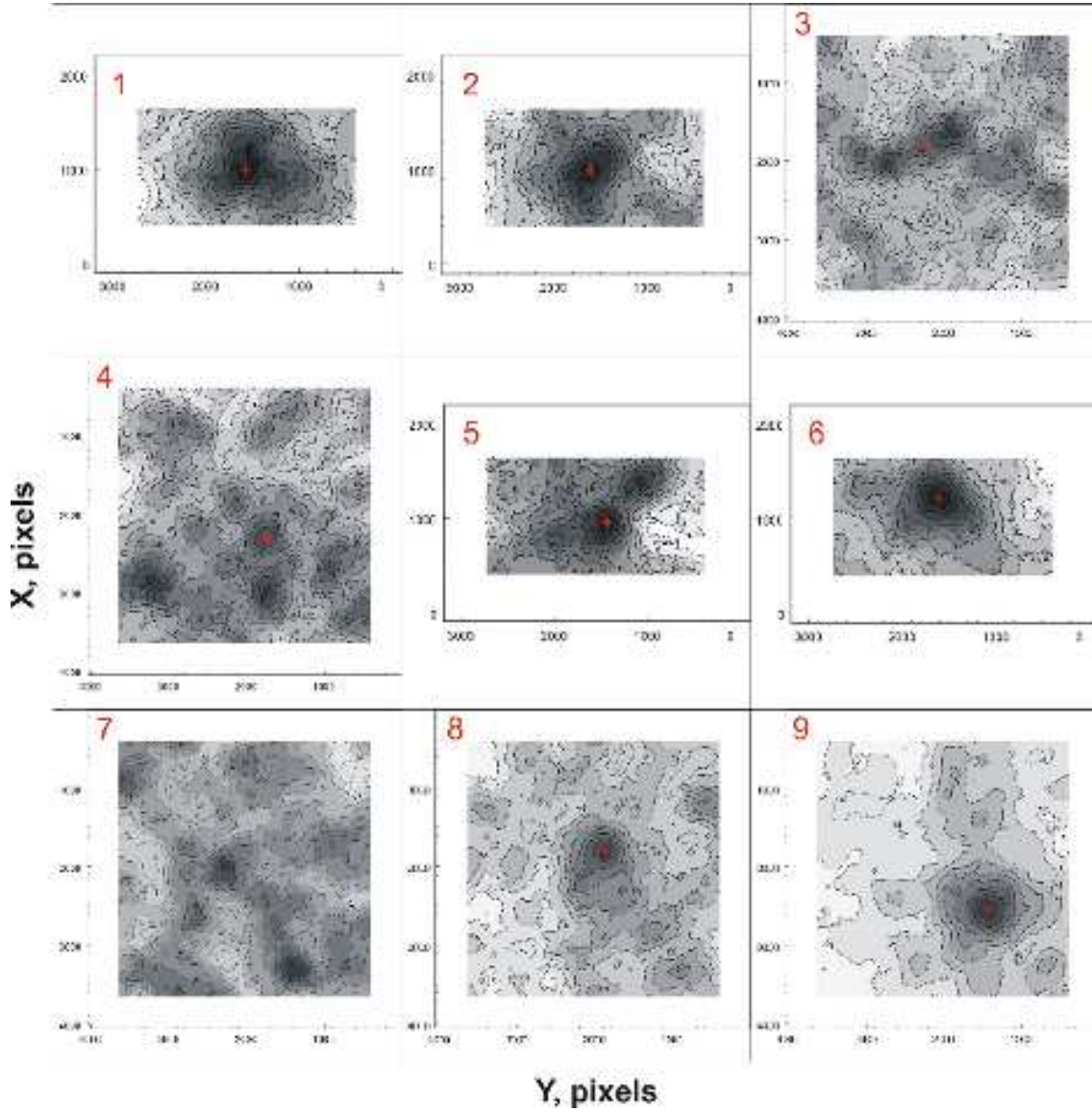


Figure 5. Optical surface density maps for the nine program clusters. North is right, East is down. Numbering follows Table 1.

of density fluctuations (to avoid, for example, numerous un-real density peaks inside a cluster), and to detect the cluster centre more clearly. Only stars brighter than a specific magnitude limit -depending on the field- were considered since the inclusion of faint stars has sometimes the effect of confusing the cluster inside the rich surrounding back/fore-ground. These limiting magnitudes are listed in Table 4.

To avoid under-sampling, we only made use of the 1240×2340 pixel ($\sim 9.0' \times 17.0'$) central region for LCO clusters and of the 3250×3250 pixel ($\sim 15.7' \times 15.7'$) central region for CTIO clusters. The resulting SDMs are shown in Fig. 5, where the iso-density contour lines are in units of $(100 \text{ pixel})^{-2}$.

New rough coordinates for the clusters' centres were obtained from the centre of symmetry of the inner (maximum) density contours. In the cases of irregular structures we estimated centre position through comparison with 2MASS density maps (see discussion below). The new cluster centres coordinates are listed in Table 5,

Table 4. Limiting magnitude for star counts in optical.

label	Name	limit in V
1	IC 2714	16
2	NGC 4052	16
3	ESO131SC09	17
4	NGC 5284	17
5	NGC 5316	16
6	NGC 5715	16
7	VdB-Hagen 164	17
8	NGC 6268	17
9	Czernik 38	19

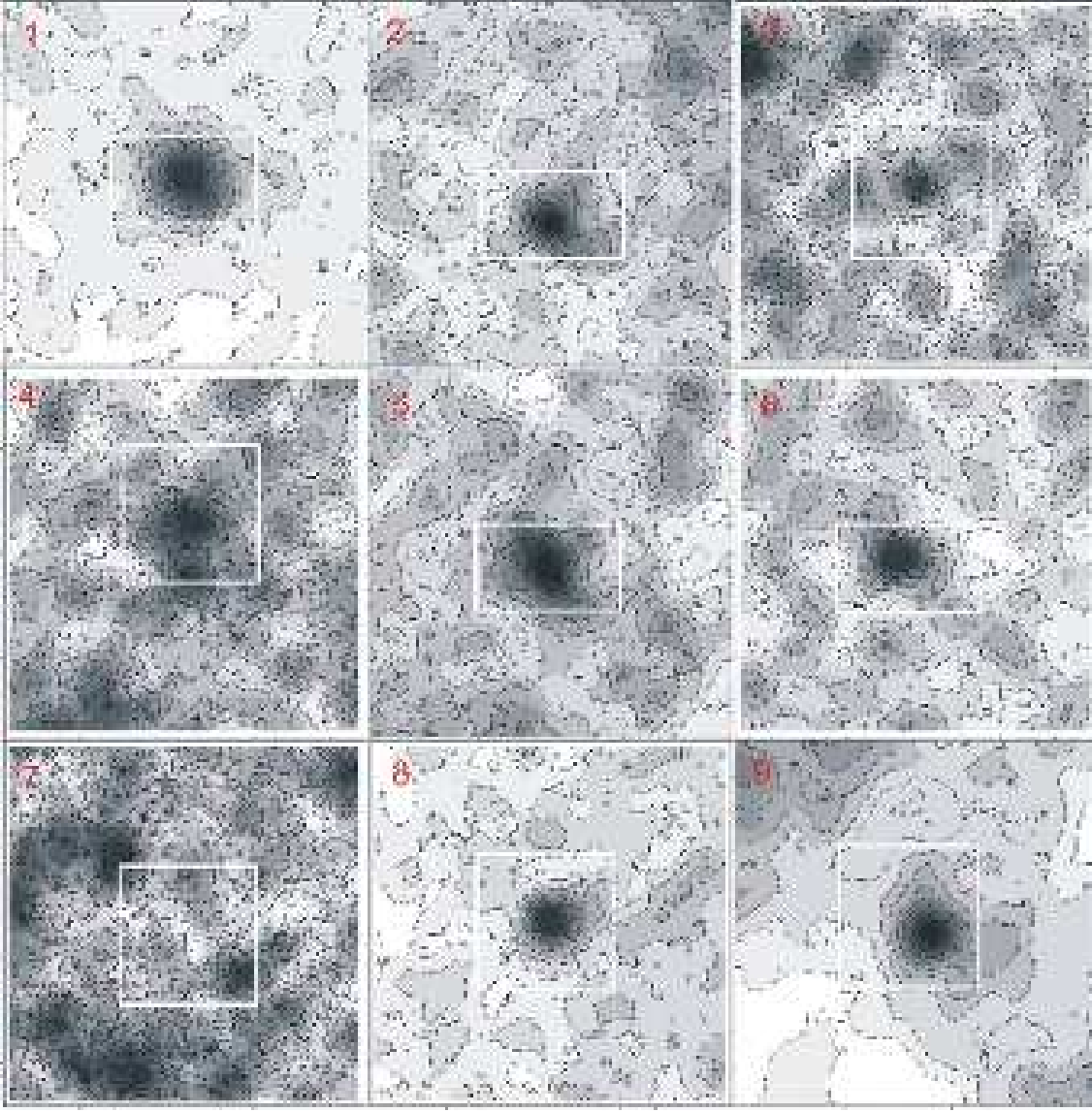


Figure 6. 2MASS Surface density maps for the nine program clusters. North is right, East is down. White boxes enclose the area covered by optical data. Numbering follows Table 1.

and they are indicated by crosses in Fig. 5. We emphasize that the use of more sophisticated methods for cluster centre determination would not make much sense in this case, because the position of the cluster centre clearly depends both on limiting magnitude and on kernel half-width. Table 5 also contains rough estimates of radii for the denser central regions of the clusters (*cores*).

One can clearly notice that in most cases the cluster size is larger than the detector field of view or just comparable to it. Therefore, in order to study the cluster structure in larger areas, to plot density profiles, and to estimate cluster sizes, we made use of star counts of photometry from the 2MASS data-base.

5.2 2MASS Surface Density Maps and Radial Surface Density Profiles for Sample Clusters

Nine fields 3600x3600 arcsec (boxes) centered on clusters were downloaded from 2MASS data-base. These fields contain huge amounts of stars and SDM plotted taking into account all stars to show density fluctuations which mask the clusters completely. In order to make clusters more evident, SDM were plotted for stars selected on color-magnitude diagrams (CMD). Stars were selected into intervals $(J-H) \simeq \pm 0.15$ wide around the position of isochrones' set super-imposed on the CMD and using preliminary values of reddening and distance modulus, mostly based on visual inspection.

SDM's obtained with kernel half-width of 5 arcmin and a grid of 0.5-arcmin cells are shown in Fig. 6. Limiting magnitudes of stars were selected in order to make clusters as visible as possible, and

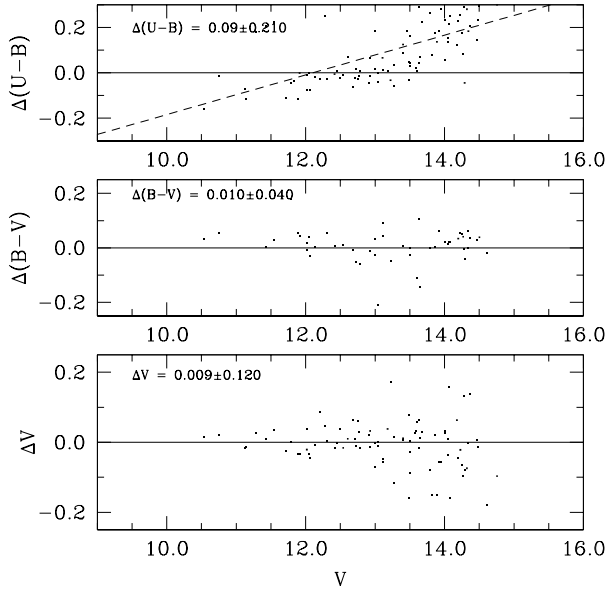


Figure 4. Comparison of our photometry for IC 2714 with Clariá et al. 1994 for V, B-V, and U-B. The comparison is in the sense of our photometry versus theirs.

Table 5. Center coordinates and core radii in pixels of the nine clusters under study.

label	Name	X_c	Y_c	"core" radius	comments
		pixels	pixels	pixels	
1	IC 2714	1000	1570	1000	
2	NGC 4052	1000	1600	800	
3	ESO131SC09	1860:	2280:	900	two centers
4	NGC 5284	2300:	1720:	1050	complicated structure
5	NGC 5316	950	1450	800	
6	NGC 5715	1200	1600	600	
7	VdB-Hagen 164	-	-	-	
8	NGC 6268	1800	1830	600	
9	Czernik 38	2550	1450	700	

these limiting magnitudes are listed in the Table 6 (third column).

To guide the reader, white rectangles in Fig. 6 shows position and extent of optical fields of view. These positions were obtained by cross-identification of the brightest stars in the optical and infrared fields. All clusters clearly stand out except for VdB-Hagen 164. This cluster from the list of van den Bergh and Hagen (1975), if real, is probably very poorly populated, close, very sparse with an angular size of supposedly much more than one degree. The data we have analyzed, however, do not give us the impression of a cluster, and therefore we are going to consider it as a false detection in this paper (see the following Sections).

SDM for all the clusters were obtained for different limiting magni-

Table 6. Limiting magnitudes for density maps from 2MASS.

label	Name	SDM limit in J	RSDP limit in J
1	IC 2714	13	15
2	NGC 4052	13	16
3	ESO 131	12	14
4	NGC 5284	13	15
5	NGC 5316	13	15
6	NGC 5715	13	16
7	BH 164	13	
8	NGC 6268	13	16
9	Cz 38	15	16

tudes. A close analysis of these maps shows that the cluster center position depends on limiting magnitude. Table 7 shows coordinates of 2MASS fields and cluster center positions with respect to field center (telescope pointing): $\alpha_c = \alpha + \Delta\alpha$, $\delta_c = \delta + \Delta\delta$ (corrections are given in arcminutes). Each limiting magnitude corrections are given in the order of $\Delta\alpha/\Delta\delta$.

Radial Surface Density Profiles (RSDP) - $F(r)$ - were then obtained by using the kernel method, and adopting a kernel half-width of 2 arcminutes. The kernel size was adjusted to avoid both extra smoothing and extra irregularities. RSDP are showed in Fig. 7 as solid curves with points. Solid curves show 1- σ confidence interval and is obtained using a "smoothed bootstrap" algorithm (see *e.g.* Seleznev et al. (2000) and Prisinzano et al. (2001) for additional details). Solid polygonal lines shows density histograms with steps of one arcmin. The adopted limiting magnitudes for RSDP are listed in the fourth column of Table 6. Finally, $F(r)$ is shown in units of $(\text{arcmin})^{-2}$.

By inspecting Fig. 7 in details, one can notice the small values of $F(r)$ at the cluster centres' position in a few cases. These are due to irregularities in the field caused, in some cases, by patchy extinction and/or field density fluctuations. Technically, the reason is that the cluster centres were determined from SDMs constructed with a large kernel half-width (5 arcmin), whereas the RSDPs have been derived adopting smaller values for the kernel width. The smaller scale produces a fluctuating profile, and as a consequence, low density values can be obtained at the centres when $F(r)$ is constructed using small increments.

5.3 Results from the SDM and RSDP analysis

In this section we analyse the outcome of star counts on a cluster-by-cluster basis, highlighting the most important results.

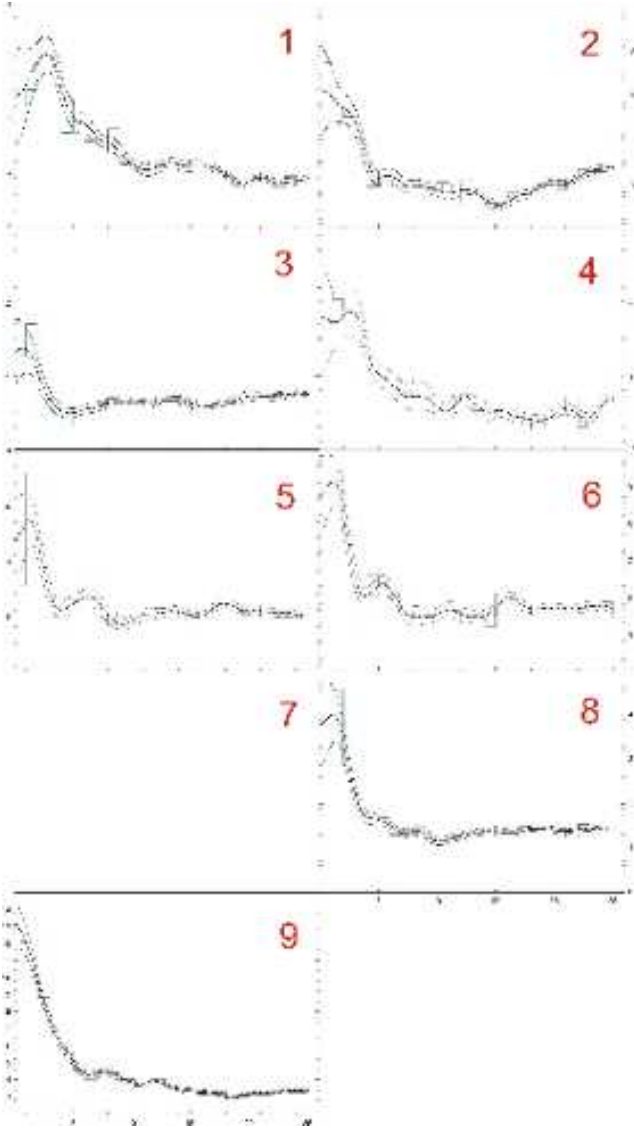
1. IC 2714

This is a rich cluster with an angular radius of about 19 arcminutes. The cluster manifests a relatively regular structure for $J_{lim} = 13$, which became more irregular for $J_{lim} = 15$. However, at $J_{lim} = 16$ (the limit of 2MASS completeness) the cluster disappears against background density fluctuations.

2. NGC 4052

Table 7. New equatorial coordinates for the clusters under investigation, obtained using 2MASS-based surface density maps.

label	Name	RA	Dec	$J < 12$	$J < 13$	$J < 14$	$J < 15$	$J < 16$	Comments
1	IC 2714	11 ^h 17 ^m 30 ^s	-62°44'00''		-0.6/+0.5	-1.0/+0.3	-0.5/+1.0		
3	ESO 131	12 ^h 29 ^m 38 ^s	-57°52'36''	+1.0/+0.5	+1.0/+0.6	+0.1/+0.6			
2	NGC 4052	12 ^h 01 ^m 12 ^s	-63°13'00''		+5.8/+0.1	+5.0/-0.1	+4.5/-0.1	+4.0/-0.5	
4	NGC 5284	13 ^h 47 ^m 23.3 ^s	-59°08'58''		-4.2/+1.1	-3.8/+0.8	-2.4/+0.5	-1.3/-2.3*	*2nd center became main
5	NGC 5316	13 ^h 53 ^m 54 ^s	-61°52'00''		+2.0/-0.7	+3.0/-0.5	+4.4/-0.1		
6	NGC 5715	14 ^h 43 ^m 24 ^s	-57°33'00''		+0.9/-2.5	+1.0/-2.5	+1.0/-2.5	0.0/-2.2	
7	BH 164	14 ^h 48 ^m 14 ^s	-66°20'23''	-	-	-	-	-	
8	NGC 6268	17 ^h 02 ^m 10 ^s	-39°43'42''		-0.3/-0.1	-0.2/+0.2	-0.1/+0.3	+0.2/0.0	
9	Cz 38	18 ^h 49 ^m 42 ^s	04°56'00''		+2.4/+2.1	+1.5/+2.0	+1.5/+2.0	+1.1/+1.8	

**Figure 7.** Surface radial density profiles for the nine program cluster. Numbering follows Table 1. No profile is shown for VdB-Hagen 164, see Section 5.

This cluster has an angular radius of about 14 arcminutes. It is well seen in the SDMs down to $J_{lim} = 14$. When including fainter stars, the cluster is still visible, but looks less populous than neighbour density fluctuations. "Optical" SDM shows a double core and an elongated outer core region.

3. ESO 131SC09

This is small group with angular radius of about 4 arcminutes. SDM shows two neighbour density fluctuations, 9 arcmin to the South, and about 8 arcmin to the North-West, respectively. To address the question whether or not they are part to the cluster, one needs additional information, *e.g.* proper motions. The *optical* SDM shows elongation of cluster roughly in the North-South direction and the presence of several density peaks. The position of cluster center was conservatively taken as the small peak just in between the two more general density peaks. In the 2MASS SDM the cluster is visible down to $J_{lim} = 14$ and disappears when including fainter stars against the background density fluctuations. Interestingly enough, the star density peak has a very low contrast with the field, the lowest in our sample. This fact may indicate that the central peak can be caused by an inter-stellar absorption minimum.

4. NGC 5284

This cluster has a complex structure. At $J_{lim} = 13$ and $J_{lim} = 14$ SDMs show a double structure with the second component 8 arcmin to the East. At $J_{lim} = 15$ this second component disappears, but we see another one 13 arcmin apart, in the North-East direction. At $J_{lim} = 16$ this component becomes prominent. The *optical* SDM also shows a complex structure with several secondary maxima. The RSDP gives an estimate of cluster radius of about 17 arcminutes.

5. NGC 5316

This cluster stands out neatly in SDM for $J_{lim} = 13$ and $J_{lim} = 14$. At $J_{lim} = 15$ cluster is still visible, but we see comparable density fluctuations around them. At $J_{lim} = 16$ the cluster disappears against the background density fluctuations. The RSDP suggests a cluster radius of about 9 arcminutes. Optical SDM shows asymmetric complex structure with at least two secondary density maxima.

6. NGC 5715

This cluster is well defined for all limiting magnitudes. At $J_{lim} = 14$ it exhibits a double structure. Neighbour density fluctuations become stronger when including fainter stars. RSDP gives a cluster radius estimate of about 8 arcminutes.

7. VdB-Hagen 164

This cluster was listed in the paper of van den Bergh and Hagen (1975). It does not possess a clear density peak either in "optical" or in "infrared" SDM. van den Bergh and Hagen (1975) write that cluster is visible in blue plates and not visible in red plates. Possibly it is a sparse group of young stars with an angular size of about a degree or even more. However, SDM plotted for a field 2x2 degrees large, do not show any density peak either.

8. NGC 6268

This cluster is clearly defined for all limiting magnitudes. Density fluctuations grow with increasing limiting magnitude and concentrate in the North-West quadrant with respect to the cluster. RSDP gives a cluster radius estimate of about 10 arcminutes.

9. Czernik 38

This is a relatively rich cluster with an angular radius of about 16-18 arcminutes. It has a symmetric core and a slightly asymmetric halo elongated in the North direction. RSDP of this cluster shows a "step" near $r=8$ arcmin.

6 FUNDAMENTAL PARAMETERS: REDDENING, DISTANCE AND AGE

In this Section we make use of the results of the star count analysis to derive estimates of the fundamental parameter, namely reddening, distance, and age for the clusters under study.

6.1 Basics of the method

We only considered the stars that fall inside the core radius, as defined in previous Sections, with the aim to alleviate as much as possible field star contamination and render the cluster more visible. The method we employed is based first on the inspection of the color-color diagram (TCD), in the B-V vs U-B color combination, to derive an independent estimate of the cluster mean reddening. In this diagram, the position of stars with spectral types earlier than A0, only depends on reddening (Carraro et al. 2008). Then, the analysis moves to the inspection of the color magnitude diagrams (CMD), in various color combinations, to derive estimates of the cluster distance and age. For the sake of homogeneity with previous studies (e.g. Seleznev et al. 2010) we adopt here $R_{\odot}=8.5$ kpc as the distance of the Sun to the Galactic center, and $R_V = 3.1$ as the ratio of total to selective absorption $\frac{A_V}{E(B-V)}$. We stress, finally, that we are going to adopt solar metallicity for these clusters, as a working hypothesis, when no information is available from spectroscopy. This is partly justified by the clusters location in the inner disk. Should solar metallicity clearly be unsuitable, we will then explore different values.

6.2 Error analysis

With the probable exception of IC 2714, most clusters in this paper are being studied for the first time. We are, therefore, facing the well-known problem of associating reliable errors to distance and

age. Without precise estimates of reddening and metallicity, it is extremely difficult to perform a proper error assessment. This would imply, in theory, a full error propagation which would in general produce a very large iper-volume in the parameters' space with many solutions which would not pass a simple by-eye inspection.

We will, therefore, limit ourselves to provide fitting errors for the cluster reddening and apparent distance moduli, being totally aware that they most probably are only rough lower limits awaiting improvements as soon as more precise metallicity measurements will be available. However, in deriving distance, a full propagation is done taking into account the whole range of values for reddening and distance modulus. Finally, as far as the ages is considered, only fitting errors are reported, adopting solar metallicity (see below).

6.3 Clusters' reddening

In Figure 8 we show the TCDs for eight of the nine program clusters. Unfortunately, we could not provide U-band photometry for Czernik 38 and therefore we are going to estimate its reddening simultaneously with age and distance from the CMD analysis, using theoretical isochrones, in a less effective way (see below). In each of the panel in Fig. 8 we show the TCD for the program clusters following their numbering as in Table 1. As anticipated, only stars within the core radius are used. The solid line is a zero reddening, solar metallicity, empirical zero age main sequence (ZAMS) taken from Schmidt-Kaler(1982). In each panel, the same empirical ZAMS is shifted along the reddening vector (indicated by the arrow in the upper-left corner) to fit the bulk of the stars in each cluster, using the green color, whenever this is possible. As for the fit, this is done by considering only the stars with spectral type earlier than A0, since for later spectral type stars there is not a unique fitting solution. To facilitate viewing, we indicated two spectral types along the ZAMS and the paths, parallel to the reddening vector, along which stars are displaced by reddening.

This procedure allows us to estimate the mean reddening for each cluster, that we report in Table 8 (third column). The associated uncertainties have been estimated visually and represent the range in reddening we can move back and forth the ZAMS keeping the fit acceptable. This uncertainty basically comes from photometric errors and variable reddening across the cluster. When the uncertainty is larger than photometric errors, which are much less than 0.03 mag in this magnitude range (see Fig 2), we are forced to conclude that differential reddening is present in the cluster. This is far from being un-expected, since these clusters are typically located at low latitude in the inner Galactic disk, inside or close to gas- and dust-rich spiral features.

6.4 Clusters' distance and age

Distances are estimated in the CMDs in Figs. 9 to 11, using the same ZAMS as in the previous Section, and adopting the reddening values already derived. In this process, therefore, distance is the only free parameter, having fixed metallicity and reddening. In the same way as for reddening, the uncertainty in distance is estimated vertically shifting the ZAMS (green line) for the range of distance moduli which provides an acceptable fit. In this process we pay attention that the reddening remains within the range of values independently estimated in the TCD.

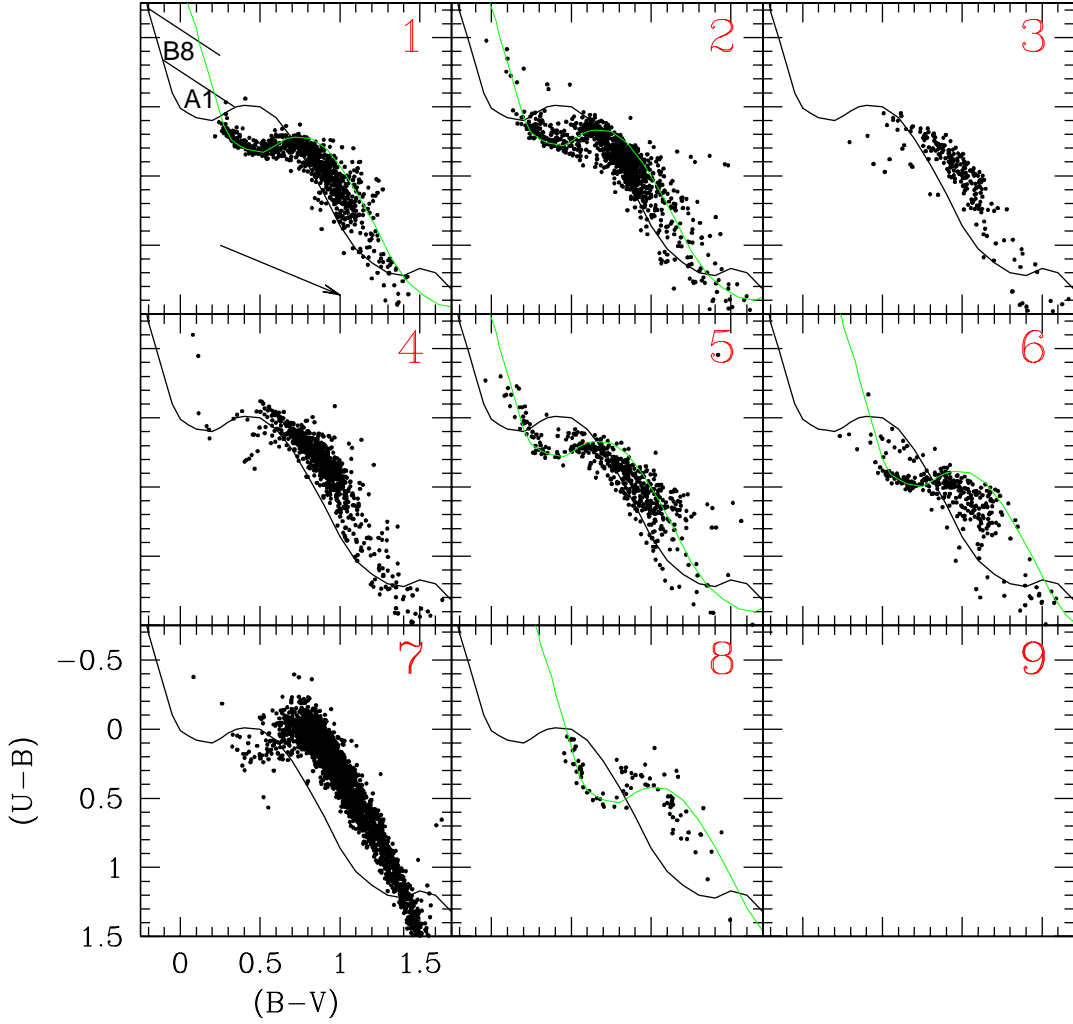


Figure 8. Color-color diagrams for the nine program clusters. The numbering follows Table 1. The solid line is an empirical zero reddening Zero Age Main sequence. The arrow in the top-left panel indicates the reddening vector. Two spectral type are indicated to guide the eye, together with the reddening path. The green line is the same ZAMS, but shifted along the reddening path by an amount corresponding to the cluster reddening $E(B-V)$.

The final step is to estimate the age, and for this we make use of isochrones from the Padova suite of models (Marigo et al. 2008, red symbols). When fitting isochrones, we pay attention to the turn off (TO) color, magnitude and shape and, when it is present, to the Red Giant clump color and magnitude. In addition, we require that the fit is of the same quality in all the three color combination CMDs.

The results are summarized in Table 8, and illustrated in Figs. 9 to 11.

7 DISCUSSION

Having detailed how fundamental parameter estimates have been searched for, we now discuss each individual cluster, commenting on the specific results. In fact, while in general a homogeneous technique has been applied, some cases, like *e.g.* Czernik 38, do

require more information.

IC 2714:

The set of fundamental parameters we found for this cluster is in fine agreement with Clariá et al. (1994) within the uncertainties, in spite of the color term problem we found when comparing their photoelectric photometry with our CCD data-set. Our results are shown in the bottom panels of Fig. 9. The TO point is located at $V \sim 12.5$, $(B-V) \sim 0.30$, and $(V-I) \sim 0.40$. A sparse red giant clump is visible at $V \leq 12.0$, $(B-V) \geq 1.2$. Santos et al. (2009) derived spectroscopic iron abundance of three giants, and provided for IC 2714 $[Fe/H] = 0.02 \pm 0.01$ and $[Fe/H] = -0.01 \pm 0.01$, depending on the line list used. In any case metallicity is very close to solar.

We, therefore, searched the solar metallicity isochrone which best fits the cluster stars distribution in the CMD, and obtained an age of $3.0 \pm 0.2 \times 10^8$ years. This implies an apparent distance modulus $(m-M)_V = 11.6 \pm 0.1$. At the corresponding helio-centric distance of $1.3^{+0.10}_{-0.15}$ kpc and ~ 40 pc below the Galactic plane,

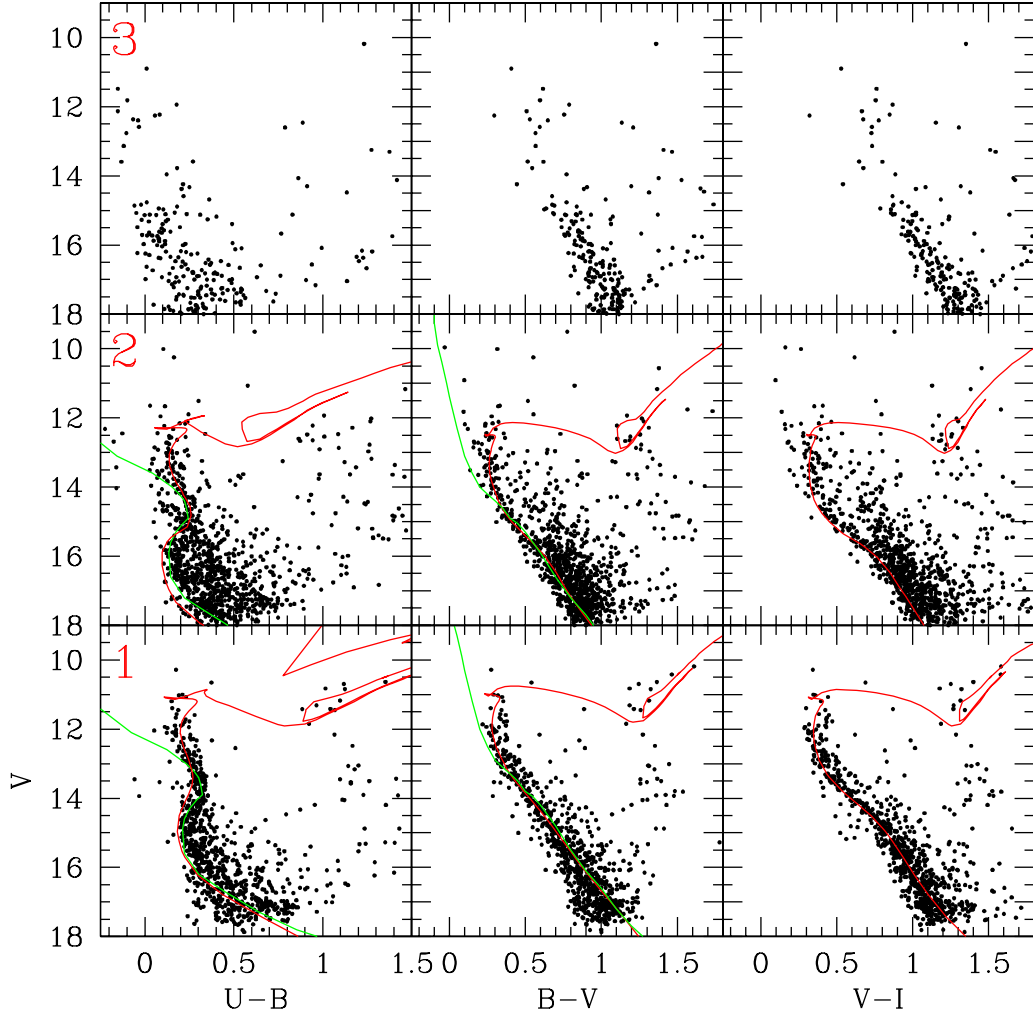


Figure 9. Color Magnitude Diagrams in the V/U-B, V/B-V, and V/V-I for IC 2714, NGC 4052, and ESO131SC09. Numbering follows Table 1. The green line is an empirical ZAMS shifted by an amount corresponding to the apparent distance modulus to fit the cluster sequence. The red lines are isochrones from Marigo et. al. 2008

IC 2714 is most probably on the act of leaving the Carina arm, where it formed. To assess this scenario, we used available literature to derive Galactic heliocentric velocities for IC 2714. The cluster has a radial velocity $R_V = -13.54 \pm 0.50$ km/sec (Mermilliod et al 2008), and UCAC2 proper motions $\mu_\alpha \cos \delta = -7.55 \pm 0.10$ and $\mu_\delta = 0.49 \pm 0.10$ (Dias et al. 2006). From these values we derived $U = 34.43 \pm 3.18$ km/sec, $V = 262.51 \pm 6.09$ km/sec and $W = 14.41 \pm 1.53$ km/sec, where U is positive toward the anticenter direction, V is positive in the Galactic rotation sense, and W points toward the North Galactic Pole. The velocities we derive imply that the cluster is moving apart from the Carina arm, drifting toward larger Galacto-centric distances.

NGC 4052:

The middle panels in Fig 9 show our results for NGC 4052, and the estimates of its basic parameters are listed in Table 8. The cluster TO is located at $V \sim 13.5$, $(B-V) \sim 0.30$, and $(V-I) \sim 0.40$, while a sparse red clump is at $V \sim 12.5$, $B-V \sim 1.2$. We fit the cluster

sequence with a solar metallicity 400 Myr isochrone, and with the Schmidt-Kaler(1982) ZAMS, which both yield an apparent distance modulus $(m-M)_V = 12.7 \pm 0.2$.

As a consequence, NGC 4052 is ubicated at $2.2^{+0.50}_{-0.30}$ kpc from the Sun, and at 7.8 kpc from the Galactic center.

ESO131SC09:

Star counts reveal the presence of a concentration of stars at the position of this object. However, from the inspection of photometric diagrams, we are keen to derive a different conclusion (see Fig 9, upper panels). Basically, we recognize two distinct groups of stars. A small number of bright blue stars in the upper region of the CMD is in fact super-imposed to a larger group of F-G stars most probably belonging to the general Galactic disk field. The two groups are clearly separated in the CMDs, and such a significant magnitude gap excludes that the two groups belong to the same system. The apparent concentration in the maps is produced by the small group of bright stars which, evidently, do

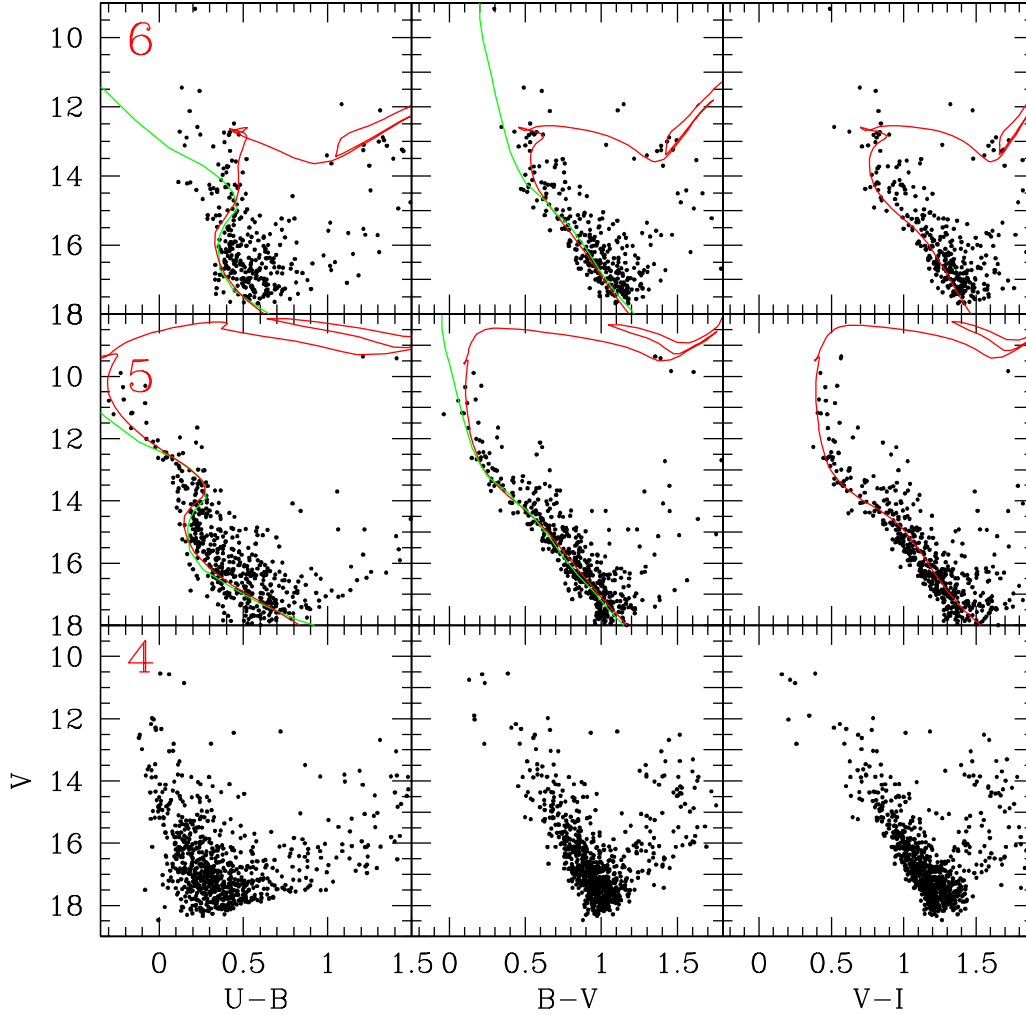


Figure 10. Color-Magnitude Diagrams in the $V/U-B$, $V/B-V$, and $V/V-I$ for NGC 5284, NGC 5316, and NGC 5715. Numbering follows Table 1. The green line is an empirical ZAMS shifted by an amount corresponding to the apparent distance modulus to fit the cluster sequence. The red lines are isochrones from Marigo et. al. 2008.

not define any stellar cluster, but, maybe, an open cluster remnant following the Loden (1973) original definition (see also Platais et al. 1998 and Carraro 2006). For these reasons we refrain from trying any isochrone fitting.

NGC 5284:

As star counts showed, this is a star agglomerate with quite a complicated structure. On DSS or CCD images, the clusters does not appear at all, and the CMDs shown in the bottom panels of Fig 10 do not show convincingly the presence of a star cluster. We believe the over-density is produced by a random concentration of a few blue stars, brighter than $V = 13$. As in the case of the previous cluster, this group looks like an open cluster remnant. In most cases, these groups do not turn out to be real clusters when proper motions or radial velocities are available to assess individual star membership to a cluster, as demonstrated by *e.g.* Odenkirchen & Soubiran (2002), Villanova et al. (2005), Carraro et al. (2005a), and Moni Bidin et al. (2010). Therefore, as in the

case of ESO131SC09, we refrain from trying any isochrone fitting.

NGC 5316:

The CMDs for this cluster are shown in the middle panels of Fig. 10. The cluster is confirmed to be a physical group of young stars, with stars having spectral types as early as B5-B7. We use the reddening estimated in Fig. 8 and fit the CMDs with solar metallicity isochrones. The best fit is achieved with an age of 100 Myrs, which, in turn, provides an apparent distance modulus $(m-M)_V = 11.50 \pm 0.20$. Therefore, we place NGC 5316 at an helio-centric distance of $1.4^{+0.15}_{-0.20}$ kpc and at a Galactic center distance of 7.6 kpc. This cluster lies very close to the formal Galactic plane, at Galactic latitude $b = 0^\circ$.

NGC 5715:

The CMDs of NGC 5715 (upper panels of Fig 10) clearly indicate it is an intermediate-age cluster, with a populated clump of RGB stars at $V \sim 13.0-13.5$, and $(B-V) \sim 1.5$. The TO is located at

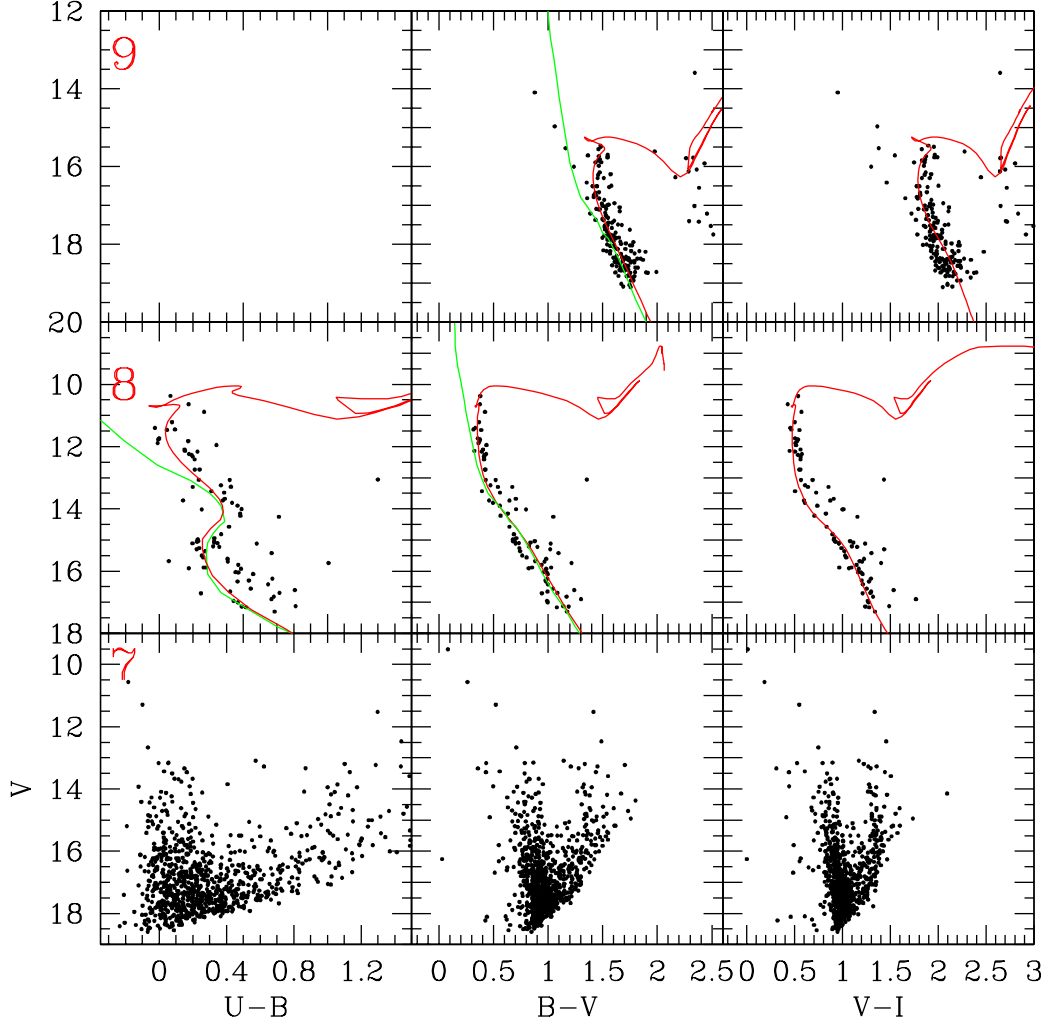


Figure 11. Color Magnitude Diagrams in the V/U-B, V/B-V, and V/V-I for VdB-Hagen 164, NGC 6268, and Czernik 38. Numbering follows Table 1. The green line is an empirical ZAMS shifted by an amount corresponding to the apparent distance modulus to fit the cluster sequence. The red lines are isochrones from Marigo et. al. 2008.

$V \sim 14.0$, $(B-V) \sim 0.5$ mag. Adopting the reddening derived from Fig. 8, we found that an 500 Myr isochrone for solar metallicity nicely follows the star distribution in all the three color combination CMDs. We estimate an apparent distance modulus $(m-M)_V = 12.75 \pm 0.20$, which translates into a distance of $1.6^{+0.8}_{-0.5}$ kpc from the Sun. NGC 5715 is thus a Hyades-like cluster located in the inner disk, similar to NGC 6583 and NGC 6404 (Carraro et al. 2005b), which apparently survived long in spite of the difficult environment of these Galaxy regions.

VdB-Hagen 164:

As already underlined in Sect. 5, there is no evidence of a star concentration neither in optical, nor in infrared at the nominal position of this object. The absence of a star cluster is also obvious when inspecting CMDs (See Fig 11, lower panels), since no clear sequences are seen in any of the diagrams. We conclude then that VdB-Hagen 164 is not a star cluster, but a random concentration of a few bright stars. As in the case of ESO131SC09 and NGC 5284,

we, therefore, refrain from trying any isochrone fitting.

NGC 6268:

This looks like a small, compact, and young cluster. The two color diagram reveals stars of spectral type as early as B2. Using the reddening derived from this diagram, we fit the star distribution in the CMDs using a 150 Myr, solar metallicity, isochrone, using the same distance modulus as for the empirical ZAMS. The TO is located at $V \approx 11.5$, $(B-V) = 0.3$ and $E(V-I) = 0.4$ mag. There is no indication of an RGB clump. The fit looks fine, and yields an apparent distance modulus $(m-M)_V = 11.4 \pm 0.2$, which implies an helio-centric distance of $1.07^{+0.20}_{-0.10}$ kpc. The cluster is about 20 pc above the plane, and 7.1 kpc from the Galactic center. Its position is compatible with it being part of the Carina-Sagittarius arm.

Czernik 38:

As commented before, we did not take U-band observations for this cluster, since it looked to be heavily reddened. The CMDs are

shown in the upper panel of Fig. 11. The TO is located at $V = 16.5$, $(B-V)=1.4$, and $(V-I) \sim 1.7$. A group of red stars at $V \sim 17.0$ seemingly indicates the presence of a RGB clump. We derived distance, age and reddening simultaneously by fitting a 600 Myr, solar metallicity, isochrone, which nicely follows the star distribution in the CMD. This fit returns a reddening $E(B-V)=1.35\pm0.15$, and an apparent distance modulus $(m-M)_V=15.30\pm0.20$. Therefore, we position Czernik 38 at $1.9^{+0.55}_{-0.40}$ kpc from the Sun and at 7.2 kpc from the Galactic center, beyond the Carina-Sagittarius arm. This location explains its significant reddening. Like NGC 5715, Czernik 38 is thus a Hyades-like cluster located in the inner disk, which managed to survive longer than the mean Galactic cluster lifetime.

8 CONCLUSIONS

We have presented and discussed UBVI photometry data for nine objects catalogued as Galactic clusters, for which only limited, if any, data was available. Structural parameters and fundamental properties have been derived, and are summarized in Tables 5 and 8, respectively.

The basic goal of this work was first to assess the reality of these objects using star counts. Second, when an overdensity was detected, we looked at photometric diagrams to probe whether stars producing the overdensity would also exhibit distinctive features in the TCD and CMDs.

This allowed us to propose that VdB-Hagen 164 is most probably not a star cluster, since its stars do not define either a spatial concentration or show clear sequences in the photometric diagrams.

We arrived at quite the same conclusion for ESO131SC09 and NGC 5284 whose stars, in spite of showing some spatial concentration, do not produce any distinctive feature in photometric diagrams. The appearance of a star cluster is generated by a group of bright stars, probably physically un-correlated. They closely resemble the so-called open cluster remnants (Loden 1973; Pavani & Bica 2007) Carraro 2006), which, in the majority of cases, are found to be random accumulations of stars along the line of sight.

The remaining targets are found to be genuine, physical, star clusters. Their ages range from 100 to 600 million years. However, only two of them (NGC 5715 and NGC 6268) are very young, and their distances are compatible with the location of the Carina-Sagittarius arm (Russeil 2003). We can conclude they formed inside the arm and are *bona fide* tracers of the arm, since with such ages they could not travel much away from their birth-place.

Unfortunately, we fail to find any young cluster located beyond the Carina-Sagittarius arm in the present sample. This clearly reflects the difficulty to penetrate the arm and to see further away because of the high density of dust and gas, unless absorption holes allow to detect more distant clusters (see *e.g.* Vázquez et al. 1995; Baume et al. 2009).

The oldest clusters (Czernik 38 and NGC 5715) are particularly interesting in the context of cluster dynamical evolution and dissolution models (Lamers et al 2005), since they could survive longer than the typical open cluster life-time in a dense and hostile environment like the inner disk, where tidal forces and close encounters do not permit star clusters to survive typically more than 100-200 Myrs (Wielen 1971).

Not many clusters of this age or older are known to

be located at these Galacto-centric distances (see *e.g.* <http://www.univie.ac.at/webda/navigation.html>). This combination of age and distance is extremely useful to investigate the Galactic disk radial abundance gradient in the inner disk (Magrini et al. 2010) and its evolution through time.

Therefore, these two clusters are ideal targets for future spectroscopic follow-up to determine their metal abundances.

ACKNOWLEDGMENTS

We acknowledge the staff of CTIO and LCO, in particular Edgardo Cosgrove and Patricio Pinto, for their valuable support during the runs. The work of A.F. Seleznev has been partly supported by the ESO Visiting Scientist Program. We are very grateful to Sandy Strunk, who carefully revised the paper and helped us to improve the language. This study made use of the SIMBAD and WEBDA databases.

REFERENCES

- Baume, G., Carraro, G., Momany, Y., 2009, MNRAS, 398, 221
- Becker, W., 1960, Zeitschr. Astrophys. 51, 49
- Bonatto, C. & Bica, E. 2007, MNRAS 377, 1301
- van den Berg, S., Hagen, G.L., 1975, AJ 80, 11
- Carraro, G., Méndez, R.A., Costa, E., 2005, MNRAS, 356, 647
- Carraro, G., Dinescu, D.I., Girard, T.M., van Altena, W.F., 2005, A&A, 433, 143
- Carraro, G., Moitinho, A., Vázquez, R.A., 2008, MNRAS, 385, 1597
- Carraro, G., Costa, E., 2009, A&A, 493, 71
- Carraro, G., Vázquez, R.A., Costa, E., Perren, G., Moitinho, A., 2010, ApJ, 718, 683
- Carraro, G., 2006, BASI, 34, 153
- Claria, J.J., Mermilliod, J.-C., Piatti, A.E., Minniti, D., 1994, A&AS 107, 39
- Czernik, M. 1966, AcA 16, 93
- Dias, W.S., Alessi, B.S., Moitinho, A., Lepine, J.R.D. 2002, A&A 389, 871
- Dias, W.S., Assafin, M., Flório, V., Alessi, B.S., LÍbero, V., 2006, A&A, 446, 949
- Dobbs, C.L., Pringle, J.E., 2010, MNRAS, 409, 396
- Efremov, Yu. N., 2011, ARep, 55, 108
- Grosbol, P., Carraro, G. Beletski, Yu., 2001, The Messenger, 143, 47
- Lamers, H.J.G.L.M., Gieles, M., Bastian, N., Baumgardt, H., Kharchenko, N.V., Portegies Zwart, S.F., 2005, A&A, 441, 131
- Landolt, A.U., 1992, AJ, 104, 340
- Lépine, J.R.D., Roman-Lopes, A., Abraham, Z., Junqueira, T.C., Mishurov, Yu.N., 2011, MNRAS, 414, 1607
- Loden, L.O., 1973, A&AS, 10,125
- Kharchenko, N.V., Piskunov, A.E., Röser, S., Schilbach E., Scholz, R.-D. 2005, A&A 438, 1163
- Maciejewski, G. 2008. AcA 58, 389
- Magrini, L., Randich, S., Zoccali, M., Jilkova, L., Carraro, G., Galli, D., Maiorca, E., Busso, M., 2010, A&A, 523, 11
- Marigo, P., Girardi, L., Bressan, A., Groenewegen, M.A.T., Silva, L., Granato, G.L., 2008, A&A, 482, 883
- Mermilliod, J.-C., Mayor, M., Udry, S., 2008, A&A, 485, 303
- Moitinho, A., Vázquez, R.A., Carraro, G., Baume, G., Lyra, W., 2006, MNRAS, 368, L77

Table 8. Estimates and associated uncertainties of the fundamental parameters of the clusters under study

Number	Name	E(B-V)	$(m - M)_V$	Age	d_\odot	d_{GC}	z
		mag	mag	Myr	kpc	kpc	pc
1	IC 2714	0.33 ± 0.05	11.60 ± 0.10	300 ± 20	$1.30^{+0.10}_{-0.15}$	8.1	~ 40
2	NGC 4052	0.30 ± 0.05	12.70 ± 0.20	400 ± 40	$2.20^{+0.50}_{-0.30}$	7.8	~ 30
3	ESO131SC09						
4	NGC 5284						
5	NGC 5316	0.25 ± 0.05	11.50 ± 0.20	100 ± 10	$1.40^{+0.15}_{-0.20}$	7.6	~ 0
6	NGC 5715	0.55 ± 0.10	12.75 ± 0.20	500 ± 100	$1.60^{+0.80}_{-0.50}$	7.4	~ 60
7	VdB-Hagen 164						
8	NGC 6268	0.40 ± 0.03	11.40 ± 0.20	150 ± 10	$1.07^{+0.20}_{-0.10}$	7.1	~ 20
9	Czernik 38	1.25 ± 0.10	15.30 ± 0.20	600 ± 100	$1.90^{+0.55}_{-0.40}$	7.2	~ 80

- Moni Bidin, C., de la Fuente Marcos, R., de la Fuente Marcos, C., Carraro, G., 2010, A&A, 510, 44
- Odenkirchen, M., Soubiran, C., 2002, A&A, 383, 163
- Pancino, E., Seleznev, A.F., Ferraro, F.R., Bellazzini, M., Piotto, G., 2003, MNRAS, 345, 683
- Patat, F., Carraro, G., 2001, MNRAS, 325, 1591
- Pavani, D., Bica, E., 2007, A&A, 468, 139
- Platais, I., Kozhurina-Platais, V., van Leeuwen, F., 1998, AJ, 116, 2423
- Prisinzano, E., Carraro, G., Piotto, G., Seleznev, A.F., Stetson, P.B., Saviane, I., 2001, A&A, 369, 851
- Ramin, M.A., 1966, AN 289, 41
- Russeil, D., 2003, A&A, 397, 133
- Santos, N.C., Lovis, C., Pace, G., Melendez, J., Naef, D., 2009, A&A, 493, 309
- Seggewiss, W. 1968, Zeitschr. Astrophys. 18, 142
- Seleznev, A.F., Carraro, G., Costa, E., Loktin, A. V., 2010, New Astronomy, 15, 61
- Schmidt-Kaler Th. 1982, Landolt-Börnstein, Numerical data and Functional Relationships in Science and Technology, New Series, Group VI, Vol. 2(b), K. Schaifers and H.H. Voigt Eds., Springer Verlag, Berlin, p.14
- Shaller, G., Schaerer, D., Meynet, G., Maeder, A., 1992, A&AS, 96, 269
- Silverman, B.W., 1986, Monographs on Statistics and Applied Probability, London: Chapman and Hall, 1986
- Smiljanic, R., Gauderon, R., North, P., Barbuy, B., Charbonnel, C., Mowlavi, N., 2009, A&A, 502, 267
- Stetson, P.B., 1987, PASP, 99, 191
- Trumpler, R.J., 1930, PASP, 42, 214
- Twarog, B.A., Ashman, K.M., Anthony-Twarog, B.J., 1997, AJ 114, 2556
- Vázquez, R.A., Baume, G., Feinstein, C., Nunez, J.A., Vergne, M.M., 2005, A&A, 430, 471
- Vázquez, R.A., May, J., Carraro, G., Bronfman, L., Moitinho, A., Baume, G., 2008, ApJ, 672, 930
- Villanova, S., Carraro, G., de la Fuente Marcos, R., Stagni, R., 2004, A&A, 428, 67
- Wielen, R., 1971, A&A, 13, 309